Computational Nonlinear Dynamics: An Assessment of Optimal Control of COVID-19 in Akwa Ibom State, Nigeria

Abstract

World Health Organization(WHO) instigates a continuous alertness and preparation to contain re-emergence of other variants of corona viruses. In the same vein, public welfare managements in allocating health related resources require predictive decision making, made possible through the assessment of existing health challenges. Therefore it is imperative to carryout an efficiency analysis to prioritize and determine an optimal control strategy that curtailed the transmission of COVID19 in Akwa Ibom state. In this paper, a deterministic epidemic model has been formulated using principles of Mathematical modelling of infectious diseases. This is a nonlinear system of differential equations coupled with three (3) time-varying control functionals. The control functionals are flexible educational programmes, vaccination and treatment of COVID-19. The usual fuzzy-like characterization of infection severity ($0 \leq R_0, R_c \leq 1$) or ($R_0, R_c > 1$) was achieved using the Next Generation Matrix Operator. An optimality system was derived using Pontryagin's Maximum principle, with some propositions on controllability criteria. Some forward-backward numerical solutions was executed in maple16 using validated datasets published by the Nigeria Centre for Disease Control(NCDC), peculiar to Akwa Ibom State. The efficiency analysis predicted that strategy I (a combination of educational intervention programmes and vaccinations of the exposed and susceptible individual) as the most efficacious and optimal control strategy. Comparatively, Strategy 1 with 96% efficiency on reducing the infected sub-population is more effective than strategy 4 (a combination of the three control states) with efficiency index of 91%. A continuous vaccination and educational awareness programme has been recommended for community health practitioners, and compliance to these policies by the citizens can eradicate the dreaded pandemic with minimal intervention cost in the state.

Key words: COVID-19, educational programme, optimal control, vaccination, and treatment

1.0 Introduction

In late 2019, the outbreak of a contagious disease; corona virus (COVID-19) in Wuhan, Hubei Province of China rooted from corina-viruses (COVs) family of coronaviridae, became a pandemic. This instigated severe health and economy challenges to human survival as the disease spread sporadically in a global scale. In etiological perspective, the four subgroups of Coronaviridae are alpha (αCoV), beta (βCoV), gamma (γCoV), and delta (δCoV). δCoV and γ CoV have avian genetic origin while the genetic origin of αCoV and βCoV have been found to be bats. COVID-19 has been likened to Severe Acute Respiratory Syndrome Coronavirus-2 (acronym SARS-CoV-2), and Middle East Respiratory Syndrome (MERS-COVs)[37]. In a microscale, it can be visualized as an enclosed nucleolytic viruse and characterized by club-like spikes from its extended surface, with special mechanism for mutation and replication with RNA genomics feature[33]. Recently, a new variant of the virus emerged as omicron, EG.5 and other variants of Interests (VOIs). The EG.5 variant poses a low

risk, as declared by WHO, but yet to detected in Nigeria. It has not been linked to a variations in symptoms as well as clinical features and has not produced an increase in severity of illness and hospitalisations or difference in death rates, in comparison to others. The transmission and transfer of the infection among humans are numerous and dynamics. These includes but not limited to inhaling and exhaling air particle in proximity to the infected person or within a cluster of persons infected with the virus, contact with surfaces, splashes and sprays infected with the virus. The infection can also be contracted via the acts of touching objects or body parts; eyes, nose or mouth with hands that have the virus on them. There are different kinds of symptom of COVID-19 experienced by people ranging from mild to severe life-threatening emergency after a possible incubation period of about 2 to 14 days on coronavirus exposure, as guided by Nigeria Centre for Disease and Control(NCDC)[30]. Although a significant number of people with COVID-19 are asymptomatic(no symptom but infectious), or presymptomatic(infectious before completion of incubation period), others experience symptoms(infectious people after incubation period). The common and mild symptoms of omicron variant as specified by NCDC includes; (i) sore throat, (ii)runny nose, (iii)blocked (stuffy) nose, (iv) sneezing (v) cough without or without phlegm (vi)headache (vii) A hoarse voice, (viii) muscle aches and pains, and (ix) an altered sense of smell. Infected person can experience fever or chills, fatigue, and gastrointestinal issues such as nausea, vomiting, or diarrhea. On the the hand, severe symptoms that warrant emergency medical attention includes; (i) Shortness of breath or difficulty breathing (ii) Persistent pain or pressure in the chest, and (iii) Pale, gray, or blue-colored skin, lips, or nail beds. co-morbidity and prior coronavirus infections predominantly occur in adults and advanced age with immuno-compromised diseases such as Cardiovascular disease (CVD), diabetes mellitus, hypertension and chronic lung disease could experience a high risk of severe infection[21]. Comparatively, a more reliable diagnostic method of the infection is Molecular test analysis; A PCR (polymerase chain reaction) test that search for the virus genomics component and the specimens collected via nasal or throat swab or through a saliva sample are analysed. Others are Antigen (Rapid or Home) Tests and Antibody Test.

The World Health Organization had declared the outbreak of COVID-19 as a public health emergency of International concern in 30th January, 2020, and ended it with great hope on the 5th May, 2023. As of 28th August, 2023 being the last weekly edition of epidemiological update of COVID-19, WHO announced that over 1.4 million new COVID-19 cases and over 1800 deaths has been reported, with an increase of 38% and a decrease of 50%, respectively, in six regions when compared to three weeks before this report [26]. Globally, as at 28th August, 2023, the World Health Organization reported that the infection had killed over 6.9 million people, with over 769 million confirmed cases. Regionally, the number of new cases and death toll in Africa keep decrease by 84% and 75% respectively as at 27th August, 2023. In Nigeria there has been no death case recorded in 2023, but since the first case was recorded on the 27th February 2023, a cumulative of 266,313 confirmed cases and 3,155 deaths cases (case fatality rate (CFR) of 1.2%) has been recorded. Specifically, in Akwa Ibom state a total of 4,976 confirmed cases and 44 deaths cases has been recorded (Nigeria Centre for Disease and Control [NCDC], 2023).

In Akwa Ibom state, there has been several intervention strategies to reduce the spread of the infection. These ranges from partial lockdown policy; reducing the infectivity of the disease via closure of schools, churches, mosques, market place, and business premises, as well as restriction of international flight to and fro the state[18]. There has been Flexible Educational Programmes(FEPs) to create awareness for the citizenry on the danger of not following the roles as stipulated by NCDC to curtail the spread [11]. These includes adherence to the use of non-pharmaceutical and personal protective equipment (PPEs) tools, such as face mask, face shields, use of hand sanitizers, nose-masks and others. Other precautionary measures were taken, but Vaccination-Treatment Approach(VTAs) breeds another face of effective intervention [2]. Several drugs including chloroquine and tradomedicine were reported to be effective to boast herd immune system and suppress the viral load in the body[23]. Vaccines utilized in Nigeria and Akwa Ibom state include (i) viral vector vaccines; (AstraZeneca-like),

and J&J-like and (ii) mRNA vaccines (Moderna- Pfizer-BioNTech-like) [35]. In one hand, for further preparation of the long COVID as envisaged by WHO, it is pertinent to assess the efficacy and cost-effectiveness analyses of these interventions, implemented to reduce and eradicate the virus. On the other hand, Mathematical modelling become a veritable to assess the optimal control strategy, utilized during the pandemic outbreak [22].

Mathematical modelling becomes a veritable tool to study the qualitative and quantitative dynamical behaviour of physical systems. The notion of Mathematical modelling has become a transdiciplinary research tool, to investigate complexities and nonlinear behaviour in several disciplines and subject including population dynamics of ecological species [14, 13, 13, 12], neuronal dynamics and cognition [4, 19], romantic love [38], drug abuse and alcohol [1, 5, 34] , terrorism and insurgency[3], finance and management sciences [36], and infectious diseases and control [24, 29]. Mathematical modelling has been used to study the spread, and control measure of infectious diseases, to facilitate sound, critical decision and policy making by the government, and other stakeholders. Being quipped with the knowledge and qualitative dynamics of the spatio-temporal behaviour of infectious diseases and pandemic helps in providing treatment options, and prevention strategies. Mathematical model assists the stakeholders to plan, evaluate, and modify numerous programs of detection. An optimal control strategy has been use to investigate a third wave of COVID-19 to reduce the disease burden on the citizens in Nigeria [25]. The simulated results showed that the presence of optimal control parameters leads to significant reduction in the impact disease. It was reported that the success of controlling the spread the infection, depends on the the implementation of the optimal control strategy. Using optimal control technique, a cost effectiveness analyses was carried [15], and the study revealed that the optimal and less costly strategy to minimize the disease is combination of vaccination and treatment of infected. In a much more realistic scenario, an optimal control and a comprehensive cost effectiveness was investigated [6]. They enlisted four (4) control and time dependent functions, namely; (i)-practising physical or social distancing protocols; (ii)-practising personal hygiene by cleaning contaminated surfaces with alcohol-based detergents; (iii)-practising proper and safety measures by exposed, asymptomatic and symptomatic infected individuals;and (iv)-fumigating schools in all levels of education, sports facilities, commercial areas and religious worship centres. They observed that the act of practising physical and social distancing among the citizens are the most cost preserving strategy to curtail the spread of the infection in the absence of vaccination. In a similar reasoning, this study localizes the notion of optimal control strategy, to assess, identify and predicts an optimal-cost effective strategy, implemented to curtail the spread of the virus in Akwa Ibom state, Nigeria.

2.0 Optimility Sytem for Control of COVID-19

This section develops an affine time-invariant dynamical system to model an optimal control of COVID-19 pandemic. In this case, the dependence on the control in the objective functional takes a positive definite quadratic function with time-varying co-state variable (Langragian multipliers) over a fixed time interval. Adoption of this control approach, enables the Hamiltonian to become strictly convex in the control state, with a unique minimizer.

2.1 Formulation of Optimal Control Problem for COVID-19

In this subsection, a nonlinear time varying system is developed with mutually exclusive compartment of human sub-population. These are susceptible class; $S(t)$, exposed class; $E(t)$, symptomatic infected class; $I(t)$, asymptomatic class; $A(t)$, hospitalized class of individuals; $H(t)$, and recovered class of individuals; $R(t)$. There are three(3) time dependent control functions, namely; (i) $u_1(t)-$flexible educational programmes; this connotes interventions to create awareness on the use of non-pharmaceutical measures or personal protective equipment (face masks, hand sanitizer, practices of social and physical distancing, practices of personal isolation strategies). (ii) $u_2(t)-$ reduction of

first wave of the infection through vaccination among the exposed, infected and asymptomatic persons. (iii) $u_3(t)-$ treatment of the infection received by hospitalized(active cases). The controls are considered as fuzzy parameter lying in the interval, $[0, 1]$. The controls vanishes at zero(0), which means that no extra measures were implemented to reduce the infection. Its takes value close to one (1) to indicates almost perfect control of the disease. The model can be represented diagrammatically as follows:

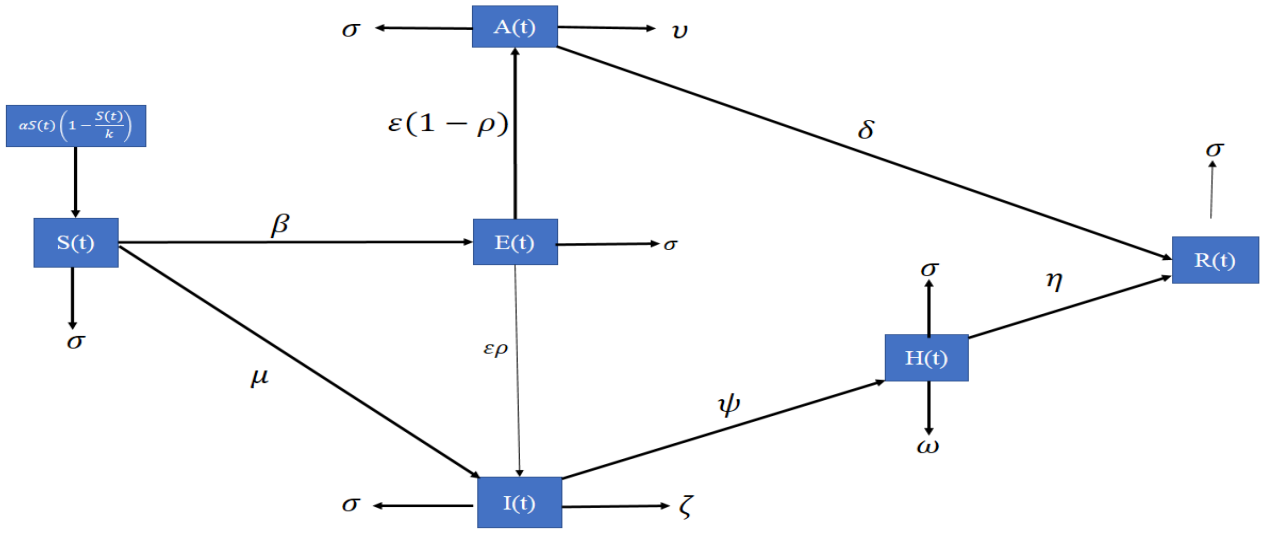

Figure 1: A compartmental representation of transmission and transition dynamics of COVID-19

The qualitative and quantitative behaviour of the model is described using in the following system of first order differential equation:

$$\begin{cases} \frac{dS}{dt} = & \alpha S(t)\left(1-\frac{S(t)}{\kappa}\right) - \beta(1-\xi u_1(t))S(t)E(t) - \mu(1-\varrho u_2(t))S(t)I(t) - \sigma S(t) \\ \frac{dE}{dt} = & \beta(1-\xi u_1(t))S(t)E(t) - (\sigma+\varrho u_2(t))E(t) \\ \frac{dI}{dt} = & \mu(1-\varrho u_2(t))S(t)I(t) + \varepsilon\rho E(t) - \psi I(t) - (\zeta+\sigma+\varrho u_2(t))I(t) \\ \frac{dA}{dt} = & \varepsilon(1-\rho)E(t)) - \delta A(t) - (\nu+\sigma+\xi u_1(t)+\varrho u_2(t))A(t) \\ \frac{dH}{dt} = & \psi I(t) - \eta H(t) - (\omega+\sigma+\epsilon u_3(t))H(t) \\ \frac{dR}{dt} = & (\delta+\xi u_1(t)+\varrho u_2(t))A(t) + (\eta+\epsilon u_3(t))H(t) - \sigma R(t) + \varrho u_2(t)I(t) \\ N(t) = & S(t)+E(t)+A(t)+I(t)+H(t)+R(t) | (S(t),E(t),A(t),I(t),H(t),R(t)) > 0 \\ & S(t)=S_0, E(t)=E_0, A(t)=A_0, I(t)=I_0, H(t)=H_0, R(t)=R_0, \forall\ t \geq 0 \\ & S_0>0, E_0>0, A_0>0, I_0>0, H_0>0, R_0>0 \\ \Omega = & \left(\mathcal{X}=(S(t),E(t),A(t),I(t),H(t),R(t))^T\right) \in \mathbb{R}^6_+ | 0 \leq N(t) \leq N_{max} \end{cases} \tag{2.1}$$

with an objective cost functional given as

$$\mathcal{J}(\mathcal{X}^*,\mathcal{U}) = \int_0^T \left(A_1E(t) + A_2I(t) + A_3H(t) + \frac{1}{2}\sum_{i=1}^{3} B_i u_i^2 \right) dt, \tag{2.2a}$$

$$\mathcal{X}^* = (E(t), I(t, H(t))\ )\ \forall \mathcal{U} = u_i \in [0, 1-\epsilon^*],\ \epsilon^* \ll 1\, i = 1, 2, 3. \tag{2.2b}$$

Then an optimal control with admissible state solution $u_i^* \in [0, 1-\epsilon^*]$ is required to minimize the total cost incured to control the spread of the infection among the transmissible subpopulations; exposed class, $E(t)$, infected class, $I(t)$, and hospitalized class $H(t)$, and defined as follows:

$$\begin{cases} \mathcal{J}(\mathcal{X}^*, u_1^*(t), u_2^*(t), u_3^*(t)) = \ \min J(u_1(t), u_2(t), u_3(t)) \\ u_i(t) \in \Omega_{\epsilon^*} \subset \left(L^{p(1\leq p<\infty)}[0,T]\right) : 0 \leq u_i(t) \leq 1-\epsilon^*,\ \epsilon^* \ll 1; \forall\, i = 1, 2, 3;\ \text{and} \end{cases} \tag{2.3}$$

which satisfies system 2.1, equations 2.2a The model can be represented in a flow diagram given in figure 1, and parameters are described in table 1.

Table 1: Epidemiologic descriptions of variables and parameters in the model

Meaning	*	Meaning	*
Susceptible class	$S(t)$	Exposed to infected (transition)	ρ
Exposed class	$E(t)$	Susceptible to exposed (transmission)	β
Infected class	$I(t)$	Susceptible to infected (transmission)	μ
Asymptomatic infected class	A(t)	Exposed to asymptomatic (transition)	ε
Hospitalized class	$H(t)$	Hospitalized to recovery (transition)	η
Recovered class	$R(t)$	Asymptomatic to recovery (transition)	δ
Educational intervention state	$u_1(t)$	Infected to hospitalized(transition)	ψ
Vaccination intervention state	$u_2(t)$	Disease induced death (Asymptomatic)	ν
Treatment intervention state (hospitalized)	$u_3(t)$	Disease induced death (infected)	ς
Disease induced death (hospitalized)	ω	Natural birth rate	α
Natural death rate	σ	Balancing cost weight (Exposed)	A_1
Max. number of susceptible individuals	κ	Balancing cost weight (Infected)	A_2
Relative intervention cost (Exposed)	B_1	Balanced cost rate (Hospitalized)	A_3
Relative intervention cost (Infected)	B_2	Intervention control rate (Educ., prog.)	ξ
Relative intervention cost (Hospitalized)	B_3	Intervention control rate (Vacc.)	ϱ
Intervention control rate (Treatment)	ϵ		

* parameter

2.2 Functional Analytics for Existence of Optimal Control of COVID-19

The existence of an optimal control function stated in equation 2.3 has been discussed extensively in related literature [10, 6] and is adapted using tools from Functional Analysis in the present study. The following theorem guarantees the existence of optimal control problem in COVID-19 established in systems 2.1 and 2.2a respectively.

Theorem 1: *There exist an optimal control functional $\mathcal{U}(u_1^*, u_2^*, u_3^*)$ defined in equation 2.3 with corresponding state solution $\mathcal{X}^*(E^*, I^*, H^*)$ to the system 2.1 which minimizes the optimization functional defined in equation 2.3 over a Lebesgue's measurable set Ω_{ϵ^*}, satisfying the following convexity conditions;*

- *i All the state variable, initial conditions as well as the control variables are non-negative values and non-empty.*
- *ii The state system 2.1 is a linear function of the control variables with coefficients dependent on time and state variables whose solution exist.*
- *iii The control set Ω_{ϵ^*} is convex and closed.*
- *iv The integrand of the objective functional 2.2a is convex on Ω_{ϵ^*}.*

Proof:

Firstly, it is straight forward to show that all solutions $\mathcal{X} = (S(t), \dot{E}(t), I(t), A(t)H(t), R(t))^T \in \mathbb{R}_+^6$ as defined in system 2.1 with positive initial conditions are uniformly bounded in the positive invariant region

$$\Omega = \left((S(t), E(t), A(t), I(t), H(t), R(t))^T\right) \in \mathbb{R}_+^6 | \, (0 \leq N(t) \leq N_{max})$$

Thus, using the first differential equation, establishes the fact that

$$\frac{dS}{dt} \leq \alpha\left(1-\frac{S(t)}{\kappa}\right) \implies \lim_{t\to\infty} supS(t) \to \frac{\kappa(\alpha-\sigma)}{\sigma}$$

Similarly, adding the sub-populations, implies that

$$\frac{dN}{dt} = \dot{S}(t)+\dot{E}(t)+\dot{I}(t)+\dot{A}(t)+\dot{H}(t)+\dot{R}(t) \leq \frac{\alpha\kappa(\alpha-\sigma)}{\sigma} - \phi_0 N(t),$$

choose $\phi_0 = min(\sigma, \nu+\sigma, \omega+\sigma, \varsigma+\sigma)$, and applying Gronwalls' inequality yields,

$$N(t) \leq \frac{\alpha\kappa(\alpha-\sigma)}{\sigma} exp(-\phi_0)t, \implies \lim_{t\to\infty} supN(t) \to \frac{\alpha\kappa(\alpha-\sigma)}{\sigma}$$

subject to initial conditions $(S_0>0, E_0>0, A_0>0, I_0>0, H_0>0, R_0>0)$.
Every solution trajectories of the flow $\mathcal{X} = (S(t), E(t), I(t), A(t)H(t), R(t))^T$ remain attracted to the feasible invariant region

$$\Omega = \left(\mathcal{X} \in \mathbb{R}^6_+ : S(t) \leq \frac{\kappa(\alpha-\sigma)}{\sigma}, N(t) \leq \frac{\alpha\kappa(\alpha-\sigma)}{\sigma} = N_{max}\right)$$

Also the the admissible control functions, were defined in a Lebesgue's Measurable set $\Omega_{\epsilon^*} \subset L^p(1 \leq p < \infty)$ and are uniformly bounded. Hence the system is bounded. Epidemiologically, the system is dissipative and meaningful. Notedly, the bounded conditions are controlled by natural growth rate (α) of the susceptible population, maximum susceptible individuals (κ) to the infection, and possible reduction in the population size through disease induced death rates (ω), and natural death rates(σ), respectively.

Secondly, the variation equation of system 2.1 can be decomposed through linearization [28] of the state variables and the controls in the neighbourhood of some isoclines $(\kappa^* > 0)$, parallel the to the disease free equilibrium; $E_0(S^* \to \kappa^*, 0, 0, 0, 0, 0) \to \mathbf{0}$. This yields a linear time varying system as follows

$$\begin{cases} \dot{\mathcal{X}}(t) = A\,\mathcal{X}(t) + B\,\mathcal{U}(t) \\ \mathcal{X}(0) = \mathcal{X}_0 \\ \text{where} \\ A = \begin{bmatrix} \alpha-\sigma-\frac{2\alpha S^*}{\kappa} & 0 & 0 & 0 & 0 & 0 \\ 0 & -\sigma & 0 & 0 & 0 & 0 \\ 0 & \varepsilon\rho & -\psi-\varsigma-\sigma & 0 & 0 & 0 \\ 0 & \varepsilon(1-\rho) & 0 & -\delta-\nu-\sigma & 0 & 0 \\ 0 & 0 & \phi & 0 & -\eta-\omega-\sigma & 0 \\ 0 & 0 & 0 & \delta & \eta & -\sigma \end{bmatrix}, \\ B = \begin{bmatrix} \beta\varepsilon S^*E^* & \mu\varrho S^*I^* & 0 \\ -\beta\varepsilon S^*E^* & 0 & 0 \\ 0 & -\mu\varrho S^*I^* & 0 \\ -\varepsilon A^* & -\varrho A^* & 0 \\ 0 & 0 & -\epsilon H^* \\ \varrho A^* & \varrho A^* + \varrho I^* & \epsilon H^* \end{bmatrix}, \end{cases} \tag{2.3a}$$

Using variation of parameter method, the analytic solution of linear system 2.3a satisfies the equation

$$\mathcal{X}(t) = \mathcal{X}_0\, exp(At) + \int_0^t exp(A(t-s))\, B\,\mathcal{U}(s)\, ds \tag{2.3b}$$

Using matrix norm,

$$|\mathcal{X}(t)| \leq \mathcal{X}_0\, exp(\|A\|t) + \int_0^t exp(\|A\|(t-s))\, \|B\|\, \|\mathcal{U}(s)\|\, ds$$

By using the definition of matrix norm on the control state and applying sylvester's theorem on the fundamental matrix solution, equation 2.3b becomes

$$|\mathcal{X}(t)| \leq \left(\sum_{i=1}^{6}\sum_{j=6}^{6} t^{i-1}\| exp\,(Re\,\lambda_i)t\|\, \|M_{ij}\|\right)\left(\mathcal{X}_0 + \max_{1\leq j\leq 6}\sum_{i=1}^{6} B_{ij}\int_0^t exp(-\|A\|s))\, \|\mathcal{U}(s)\|\, ds\right) < \infty$$

where M_{ij} is the corresponding Frobenius covariants matrices of A, with bang-bang control principle ($\|\mathcal{U}(s)\| = 1$), and real part eigenvalues of A, $Re\lambda_i \leq 0$. Also, by introducing the limit, then the control state steers the solution eqution 2.3b such that

$$|\mathcal{X}(t)| \leq \infty \quad \forall t \in [0,T], \text{and} \;\; |\mathcal{X}(t)| \to 0 \;\; as \;\; t \to \infty$$

Consequently, this proof establishes the following condition for local controllablity of system (ODE) 2.1

Corrolary 1[Controllablity Criteria [28]] The model in system 2.1 on linearization is asymptotically controllable for stable matrix A.

To establish the third condition in the theorem(convexity condition). Define the possible reachable set of initial conditions $\mathcal{X}_0 \in \mathcal{C}(t)$, and admisible control region in a measurable set say,

$$\Omega_{\epsilon^*} \subset L^{p(1\leq p<\infty)}[0,T]^3 \;=\; (\mathcal{U}(u_i^*) : 0 \leq u_i^*(t) \leq 1) \;\; \forall i = 1,\, 2,\, 3.$$

that steers the reachable set $\mathcal{C}(t)$ to 0 at all time $t \in [0,T]$. Then select points, say $p_1 = (a_1, a_2, a_3),\; p_2 = (b_1, b_2, b_3)$ in Ω_{ϵ^*}. Then it suffice to show that there exist

$$\begin{aligned} z &= p_1\lambda + (1-\lambda)p_2 \; in \; \Omega_{\epsilon^*} \;\; \text{for all } 0 \leq \lambda \leq 1 \\ &= (a_1, a_2, a_3)\lambda + (1-\lambda)(b_1, b_2, b_3) \\ &= [(a_1\lambda, a_2\lambda, a_3\lambda) + ((1-\lambda)b_1, (1-\lambda)b_2, (1-\lambda)b_3)] \\ &= a_1\lambda + (1-\lambda)b_1,\; a_2\lambda + (1-\lambda)b_2,\; a_3\lambda + (1-\lambda)b_3 \\ &= (z_1, z_2, z_3) \in \Omega_{\epsilon^*} \end{aligned}$$

Hence the condition of convexity is satisfied.

In the same vein, to establish that the integrand

$$L = A_1E(t) + A_2I(t) + A_3H(t) + \frac{1}{2}\sum_{i=1}^{3} B_iu_i^2$$

is convex, the Hessian Matrix technique is applied. The condition stipulates that, the given function is convex if the Hessian matrix defined as $H_L = \frac{\partial^2 L}{\partial u_i \partial u_j}$

$$\begin{aligned} H_L &= \begin{bmatrix} \frac{\partial^2 L}{\partial^2 u_1} & \frac{\partial^2 L}{\partial u_1 \partial u_2} & \frac{\partial^2 L}{\partial u_1 \partial u_3} \\ \frac{\partial^2 L}{\partial u_2 \partial u_1} & \frac{\partial^2 L}{\partial^2 u_2} & \frac{\partial^2 L}{\partial u_2 \partial u_3} \\ \frac{\partial^2 L}{\partial u_3 \partial u_1} & \frac{\partial^2 L}{\partial u_3 \partial u_2} & \frac{\partial^2 L}{\partial^2 u_3} \end{bmatrix} \\ &= \begin{bmatrix} B_1 & 0 & 0 \\ 0 & B_2 & 0 \\ 0 & 0 & B_3 \end{bmatrix} \geq 0 \end{aligned}$$

Since the the Hessian matrix is positive semi-definite, so the integrand is convex. Then the compactness of the set Ω_{ϵ^*} is guaranteed by Alaoglus's weak convergence theorem in L^p- space [20], and the geometric approach of Krien-Milan theorem [31] ensure extreme points. Thus for every control states $u_i \in \Omega_{\epsilon^*}$, there exist a subseqence u_{ik} and $u \in \Omega_{\epsilon^*}$ such that $u_{ik} \rightharpoonup u$, then Ω_{ϵ^*} has at least one extreme point.

2.3 Characterization of Optimal Control of COVID-19

The necessary condition for admissible control state $\mathcal{U}(u_1^*, u_2^*, u_3^*)$ to be optimal can be generated from a continuously differentiable time-varying function (adjoint), $\lambda(t)$ over an extremal set $[0, T]$ and a Hamiltonian functional ($\mathcal{H}$) defined as;

$$\begin{cases} \mathcal{H}(\mathcal{X}^*, \mathcal{U}, \lambda, t) = & \mathcal{J}(\mathcal{X}^*, \mathcal{U}, t) + \lambda(t)\mathcal{G}(X, \mathcal{U}, t); \\ & \text{where } \mathcal{G} = \dot{\mathcal{X}}(t) = \frac{\partial \mathcal{H}}{\partial \lambda} \end{cases} \tag{2.4}$$

Furthermore, the admissible control state, $\mathcal{U}(u_i^*, u_2^*, u_3^*)$ satisfies the Pontryagin's Maximum Principle[32, 17];

$$\begin{cases} \frac{\partial \mathcal{H}}{\partial \mathcal{U}} = 0 \text{ at } \mathcal{U}(u_i^*, u_2^*, u_3^*) & \text{(optimality condition)} \\ \frac{d\lambda}{dt} = -\frac{\partial \mathcal{H}}{\partial \mathcal{X}} & \text{(adjoint condition)} \\ \lambda(T) = 0 & \text{(transversality condition)} \\ \frac{\partial^2 \mathcal{H}}{\partial \mathcal{U}^2} < 0 \text{ at } \mathcal{U}(u_i^*, u_2^*, u_3^*) & \text{(maximization condition)} \\ \frac{\partial^2 \mathcal{H}}{\partial \mathcal{U}^2} > 0 \text{ at } \mathcal{U}(u_i^*, u_2^*, u_3^*) & \text{(minimization condition)} \end{cases} \tag{2.5}$$

which ensures the existence of a critical extremal functional, and transforms the control state in equation 2.3 subject to the model system 2.1 into a problem of minimizing pointwise a Hamiltonian functional, $\mathcal{H}$ defined in equation 2.4. So, the following theorem is used to to obtain the admissible controls $\mathcal{U}(u_1^*, u_2^*, u_3^*)$ as functions of the state varaibles

Theorem 2: *Given an optimal control $\mathcal{U}(u_1^*, u_2^*, u_3^*)$ and the corresponding solution $\mathcal{X}^*(S^*, E^*, I^*, A^*, H^*, R^*)$ that minimizes the objective cost functional $\mathcal{J}(\mathcal{X}^*, \mathcal{U})$ over a measurble set Ω_{ϵ^*}. Then there exists a continously differentiable function(co-state variable) $\lambda_i(t)$ $i = 1, 2, ..., 6$ that satisfies the Pontryagin's Maximum Principle. Furthermore, the admissible optimal controls are given as follows;*

$$\begin{cases} u_1^* = min\left(1, max\left(0, \phi_1\right)\right); & \phi_1 = \frac{\beta\,\xi\,S^*E^*(\lambda_2 - \lambda_1) + \xi\,A^*(\lambda_6 - \lambda_4)}{B_1} \\ u_2^* = min\left(1, max(0, \phi_2)\right); & \phi_2 = \frac{\mu\varrho\,S^*I^*(\lambda_3 - \lambda_1) + \varrho E^*\lambda_2 + \varrho I^*(\lambda_3 - \lambda_6) + \varrho A^*(\lambda_4 - \lambda_6)}{B_2} \\ u_3^* = min(1, max(0, \phi_3)); & \phi_3 = \frac{\epsilon\,H^*(\lambda_5 - \lambda_6)}{B_3} \end{cases} \tag{2.6}$$

Proof:
Explicitly, the Hamiltonian, $\mathcal{H}$ of the model is given as

$$\begin{cases} \mathcal{H} = & A_1E(t) + A_2I(t) + A_3H(t) + \frac{1}{2}(B_1u_1^2 + B_2u_1^2 + B_3u_1^2) \\ & +\lambda_1(t)\left(\alpha S(t)\left(1 - \frac{S(t)}{\kappa}\right) - \beta(1 - \xi u_1(t))S(t)E(t) - \mu(1 - \varrho u_2(t))S(t)I(t) - \sigma S(t)\right) \\ & +\lambda_2(t)\left(\beta(1 - \xi u_1(t))S(t)E(t) - (\sigma + \varrho u_2(t))E(t)\right) \\ & +\lambda_3(t)\left(\mu(1 - \varrho u_2(t))S(t)I(t) + \varepsilon\rho E(t) - \psi I(t) - (\zeta + \sigma + \varrho u_2(t))I(t)\right) \\ & +\lambda_4(t)\left(\varepsilon(1 - \rho)E(t)\right) - \delta A(t) - (\nu + \sigma + \xi u_1(t) + \varrho u_2(t))A(t)) \\ & +\lambda_5(t)\left(\psi I(t) - \eta H(t) - (\omega + \sigma + \epsilon u_3(t))H(t)\right) \\ & +\lambda_6(t)\left((\delta + \xi u_1(t) + \varrho u_2(t))A(t) + (\eta + \epsilon u_3(t))H(t) - \sigma R(t) + \varrho u_2(t)I(t)\right) \\ & +w_1(t)u_1(t) - w_2(t)(1 - u_1) + w_3(t)u_2(t) + w_4(t)(1 - u_2(t)) + w_5(t)u_3(t) + w_6(t)(1 - u_3(t)) \end{cases} \tag{2.7}$$

where $w_i(t), \forall\ i = 1, 2, ..., 6$ denotes the penalty multipliers ensuring the boundedness of the control state $\mathcal{U}(u_1(t),\ u_2(t),\ u_3(t))$ and satisfies the conditions:

$$\begin{cases} w_1(t)u_1(t) = w_2(t)(1 - u_1) = 0 \text{ at } u_1^* \\ w_3(t)u_2(t) = w_4(t)(1 - u_2(t)) = 0 \text{ at } u_2^* \\ w_5(t)u_3(t) = w_6(t)(1 - u_3(t)) = 0 \text{ at } u_3^* \end{cases} \tag{2.8}$$

Through the application of Pontryagin's Maximum Principle established in systems 2.4 and 2.5 as well as the existence result for the optimal control established in theorem 1, the adjoint (co-state) variables are defined as follows:

$$\begin{cases} \frac{d\lambda_1}{dt} = -\frac{\partial \mathcal{H}}{\partial S} = \lambda_1(t)\left(\frac{2\alpha S(t)}{\kappa} - \alpha\right) + \beta(1-\xi u_1(t))I(t)(\lambda_1(t)-\lambda_2(t)) + \mu(1-\varrho u_2(t))I(t)E(t) \\ \frac{d\lambda_2}{dt} = -\frac{\partial \mathcal{H}}{\partial E} = \beta(1-\xi u_1(t))S(t)(\lambda_1(t)-\lambda_2(t)) + \lambda_2(t)(\sigma - \varrho u_2(t)) - \varepsilon\rho\lambda_3(t) - \varepsilon(1-\rho)\lambda_4(t) \\ \frac{d\lambda_3}{dt} = -\frac{\partial \mathcal{H}}{\partial I} = \mu(1-\varrho u_2(t))(\lambda_1(t)-\lambda_3(t)) + \psi(\lambda_3(t)-\lambda_5(t)) + (\varsigma+\sigma)\lambda_3(t) + \varrho u_2(t)(\lambda_3(t)-\lambda_6(t)) \\ \frac{d\lambda_4}{dt} = -\frac{\partial \mathcal{H}}{\partial A} = (\delta + \xi u_1(t) + \varrho u_2(t))(\lambda_4(t)-\lambda_6(t)) + (\nu+\sigma)\lambda_4(t) \\ \frac{d\lambda_5}{dt} = -\frac{\partial \mathcal{H}}{\partial H} = (\lambda_5(t)-\lambda_6(t))(\eta_\epsilon\, u_3(t)) + (\omega+\sigma)\lambda_5(t) \\ \frac{d\lambda_6}{dt} = -\frac{\partial \mathcal{H}}{\partial R} = \sigma\lambda_6(t) \\ \lambda_1(T) = \lambda_2(T) = \lambda_3(T) = \lambda_4(T) = \lambda_5(T) = \lambda_6(T) = 0 \end{cases} \tag{2.9}$$

Similarly, the model satisfies the optimality condition in system 2.5; $\frac{\partial \mathcal{H}}{\partial u_1} = \frac{\partial \mathcal{H}}{\partial u_2} = \frac{\partial \mathcal{H}}{\partial u_3} = 0$ at $\mathcal{U}(u_1^*, u_2^*, u_3^*)$. Hence differentiating and simplifying the Hamiltonian leads to the following triple admissible control sets;

$$\begin{cases} u_1^*(t) = \frac{\beta\,\xi\,S^*E^*(\lambda_2-\lambda_1)+\xi\,A^*(\lambda_6-\lambda_4)+w_2(t)-w_1(t)}{B_1} \\ u_2^*(t) = \frac{\mu\varrho\,S^*I^*(\lambda_3-\lambda_1)+\varrho E^*\lambda_2+\varrho I^*(\lambda_3-\lambda_6)+\varrho A^*(\lambda_4-\lambda_6)+w_4(t)-w_3(t)}{B_2} \\ u_3^*(t) = \frac{\epsilon\,H^*(\lambda_5-\lambda_6)+w_6(t)-w_5(t)}{B_3} \end{cases} \tag{2.20}$$

Next, the standard control argument is used to eliminate the penalty functions to obtain an explicit expression for the control variables in the region Ω_{ϵ^*} as follows:

$$\begin{cases} u_1^* = \begin{cases} \phi_1 & \text{if } 0 < \phi_1 < 1 \\ 0 & \text{if } \phi_1 \le 0 \\ 1 & \text{if } \phi_1 > 1 \end{cases}, \; u_2^* = \begin{cases} \phi_2 & \text{if } 0 < \phi_2 < 1 \\ 0 & \text{if } \phi_2 \le 0 \\ 1 & \text{if } \phi_2 > 1 \end{cases}, \; u_3^* = \begin{cases} \phi_3 & \text{if } 0 < \phi_3 < 1 \\ 0 & \text{if } \phi_3 \le 0 \\ 1 & \text{if } \phi_3 > 1 \end{cases} \\ \text{where} \\ u_1^* = min\left(1, max\left(0, \phi_1\right)\right); \quad \phi_1 = \frac{\beta\,\xi\,S^*E^*(\lambda_2-\lambda_1)+\xi\,A^*(\lambda_6-\lambda_4)}{B_1} \\ u_2^* = min\left(1, max(0, \phi_2)\right); \quad \phi_2 = \frac{\mu\varrho\,S^*I^*(\lambda_3-\lambda_1)+\varrho E^*\lambda_2+\varrho I^*(\lambda_3-\lambda_6)+\varrho A^*(\lambda_4-\lambda_6)}{B_2} \\ u_3^* = min(1, max(0, \phi_3)); \quad \phi_3 = \frac{\epsilon\,H^*(\lambda_5-\lambda_6)}{B_3} \end{cases} \tag{2.21}$$

In compact notation, system 2.21 yields the admissible control triple as required. □

3.0 Dynamics of COVID-19 Reproduction Numbers

The Basic Reproduction Number; (R_0), measures on average, the spread or transmission of the infection from a single infectious individual without any control intervention. Its provides the necessary condition for epidemic trajectories and disease control strategies. On the other hand, the Control Reproduction Number; (R_c), measures the corresponding reduction in the spread or transmission of the infection in the presence of control interventions. In epidemiological perspective, the disease will follow extinction route from the population if the basic or control reproduction number is within the unit threshold; $0 < R_0,\, R_c \le 1$, otherwise it persists endemically in the population as $R_0,\, R_c > 1$. Dynamical behaviours of the model becomes self-organized with complexities and uncertainties when the reproduction numbers; $(R_0, R_c = 1)$.

3.10 Characterization of COVID-19 Reproduction Numbers

The Next Generation Operator(NGO) [27, 7], will be employed to establish the reproduction numbers of the COVID-19 model in system 2.1. These include the basic reproduction (R_0) and control reproduction (R_c) numbers respectively. The following definition gives a theoretical background for derivation of the basic reproduction numbers.

Definition: Let $\mathcal{X}$ be a Banach lattice functions $[0,1] \to \mathbb{R}$, and $X \in \mathcal{X}$ represent the state space variables. Consider a biologically meaningful and linear evolution equation of the form

$$X'(t) = AX(t) - MX(t) \tag{3.11}$$

where $B : \mathcal{X} \to \mathcal{X}$ is a linear operator to account for transmission of infectious disease, and $M : \mathcal{D}(M) \subseteq \mathcal{X} \to \mathcal{X}$ is a linear operator meant to account for transition and transfer of the infectious disease. If the following conditions as satisfied

- $A1 : A$ is positive and bounded.
- $A1 : -M$ generates a strongly-continuous semigroup $\phi_t(.) \subseteq \mathcal{X}$ of positive linear operators, with strictly negative spectral bound.

Then the basic reproduction R_0 has been characterized as the spectral radius [8] of the Next Generation Operator (NGO); $AM^{-1} : \mathcal{X} \to \mathcal{X}$ defined as

$$R_0 = \rho\left(AM^{-1}\right) \tag{3.12}$$

Additionally, under the assumptions $A1$ and $A2$, then AM^{-1} is positive and bounded, so that R_0 is a non-negative spectral value. Aslo, if AM^{-1} is compact and it has positive spectral radius, the Krein-Ruthman theorem [16] ensures that R_0 is a positive eigenvalue, i,e., a solution λ of

$$AM^{-1}\psi = \lambda\psi \tag{3.13}$$

for some (nontrivial) positive eigenfunction ψ. Equivalently, λ satisfies the generalized eigenvalue problem

$$A\phi = \lambda M\phi \tag{3.14}$$

with $\phi = M^{-1}\psi \in \mathcal{D}(M)$.

3.12 Control Interventions and COVID-19 Reproduction Numbers

Using definition 1, the model in system 2.1 can be decomposed to the following system of matrices, evaluated at the disease control equilibrium; $E_0 = \left(S_0 = \frac{\kappa(\alpha-\sigma)}{\alpha}, E_0 = 0, I_0 = 0, A_0 = 0, H_0 = 0, R_0 = 0\right)$.

$$\begin{cases} M = \begin{bmatrix} \varrho\, u_2 + \sigma, & u_2\,\varrho + \psi + \sigma + \varsigma & 0 & 0 \\ -\varepsilon\rho & \varrho u_2 + \phi + \sigma + \varsigma & 0 & 0 \\ -\varepsilon\ (1-\rho) & 0 & u_1\,\xi + u_2\,\varrho + \delta + \sigma + \upsilon & 0 \\ 0 & -\psi & 0 & \epsilon\, u_3 + \eta + \omega + \sigma \end{bmatrix} \\ M^{-1} = \begin{bmatrix} (u_2\,\varrho + \sigma)^{-1} & 0 & 0 & 0 \\ \frac{\varepsilon\,\rho}{(u_2\,\varrho+\sigma)(u_2\,\varrho+\psi+\sigma+\varsigma)} & (u_2\,\varrho + \psi + \sigma + \varsigma)^{-1} & 0 & 0 \\ -\frac{\varepsilon\,(-1+\rho)}{(u_2\,\varrho+\sigma)(u_1\,\xi+u_2\,\varrho+\delta+\sigma+\upsilon)} & 0 & (u_1\,\xi + u_2\,\varrho + \delta + \sigma + \upsilon)^{-1} & 0 \\ M_{41} & M_{42} & 0 & M_{44} \end{bmatrix} \end{cases} \tag{3.14}$$

$$\begin{cases} M_{42} = \frac{\psi\,\varepsilon\,\rho}{(u_2\,\varrho+\sigma)(u_2\,\varrho+\psi+\sigma+\varsigma)(\epsilon\,u_3+\eta+\omega+\sigma)}, \quad M_{42} = \frac{\psi}{(u_2\varrho+\psi+\sigma+\varsigma)(\epsilon u_3+\eta+\omega+\sigma)}, \quad M_{44} = (\epsilon\,u_3+\eta+\omega+\sigma)^{-1} \\ A = \begin{bmatrix} \frac{\beta\kappa\,(\alpha-\sigma)(1-\varepsilon u_1)}{\alpha} & 0 & 0 & 0 \\ 0 & \frac{\mu\,\kappa\,(\alpha-\sigma)(1-\varrho u_2)}{\alpha} & 0 & 0 \\ 0 & 0 & 0 & 0 \\ 0 & 0 & 0 & 0 \end{bmatrix} \quad AM^{-1} = \begin{bmatrix} \frac{\beta\,(1-\xi u_1\,)\kappa(\alpha-\sigma)}{\alpha\,(\varrho u_2+\sigma)} & 0 & 0 & 0 \\ \frac{\mu\,(1-u_2\,\varrho)\kappa(\alpha-\sigma)\varepsilon\,\rho}{\alpha\,(u_2\,\varrho+\sigma)(u_2\,\varrho+\psi+\sigma+\varsigma)} & \frac{\mu\,(1-u_2\,\varrho)\kappa(\alpha-\sigma)}{\alpha\,(u_2\,\varrho+\psi+\sigma+\varsigma)} & 0 & 0 \\ 0 & 0 & 0 & 0 \\ 0 & 0 & 0 & 0 \end{bmatrix} \end{cases}$$

Hence the following characteristic polynomial of the Next Generation Operator (NGO) and it corresponding eigenvalues are the required reproduction numbers.

$$\begin{cases} P(AM^{-1},\lambda) = \lambda^4 + p_1\lambda^3 + p_0\lambda^2 \\ p_1 = \frac{\kappa(\alpha-\sigma)\left(\beta\,u_1\,u_2\,\varrho\,\xi+\mu\,{u_2}^2\varrho^2+\beta\,\psi\,u_1\,\xi+\beta\,\sigma\,u_1\,\xi+\beta\,u_1\,\xi\,\varsigma+\mu\,\sigma\,u_2\,\varrho-\beta\,u_2\,\varrho-\mu\,u_2\,\varrho-\beta\,\psi-\beta\,\sigma-\beta\,\varsigma-\mu\,\sigma\right)}{\alpha\,(u_2\,\varrho+\sigma)(u_2\,\varrho+\psi+\sigma+\varsigma)} \\ p_0 = \frac{\mu\,(1-\varrho u_2)(\kappa(\alpha-\sigma))^2\beta\,(1-\xi u_1)}{\alpha^2(u_2\,\varrho+\psi+\sigma+\varsigma)(u_2\,\varrho+\sigma)} \\ R_c = \rho\,(AM^{-1}) = max\,(R_{01},R_{02})\,; \quad R_0 = max\,(R_{03},R_{04})\,, \text{ where} \\ R_{01} = \frac{\mu\,(1-\varrho u_2)\kappa(\alpha-\sigma)}{\alpha\,(\varrho u_2\,+\psi+\sigma+\varsigma)}, \quad R_{02} = \frac{\beta\,(1-\xi u_1)\kappa(\alpha-\sigma)}{\alpha\,(u_2\,\varrho+\sigma)}, \quad R_{03} = \frac{\mu\,\kappa(\alpha-\sigma)}{\alpha\,(\psi+\sigma+\varsigma)}, \quad R_{04} = \frac{\beta\,\kappa(\alpha-\sigma)}{\alpha\,\sigma} \end{cases} \tag{3.15}$$

It's easy to observe that the characterization of the reproduction numbers are epidemiologically meaningful, since $R_c \leq R_0$ for $0 < u_i^* \leq 1$, $\forall i = 1,2,3$. Hence the intervention and control strategies were of benefit to the people, and a positive impact leading to reduction of COVID-19 infections in the state.

4.0 Numerical Simulations and Discussions

For the purpose of numerical simulations, COVID-19 datasets of Akwa Ibom state as reported by the Nigeria Centre for Disease Control (NCDC) has been validated, estimated and fitted numerically, using least square technique in a similar study [9]. This study adopts same datasets to estimate unknown parameters of the model as seen in Table 2 with initial conditions for the period of ten(10) months. Some forward-backward numerical schemes in Maple16 software were used to obtain the solution profiles and phase space diagrams to validate the qualitative properties of the model established in previous sections.

Table 2: Numerical parameters and variables

Parameters	α	β	μ	η	ϱ	ξ	ω	ν	ς	ρ	κ	ψ	ε	δ	σ
Values	0.7	0.75	0.5	1.5	0.8	0.7	0.5	0.22	0.02	0.98	10	0.5	4.5	.053	0.6

Parameters	ϵ	A_1	A_2	A_3	B_1	B_2	B_3
Values	0.5	1	1	1	20	20	20

4.10 Impacts of Control Interventions on COVID-19 Reproduction Numbers

Using system 3.15 and values of the model parameters in table 2. It's worthwhile to observe that the values of different parameter changes the magnitude of R_c, and R_0 which ultimately reflect the severity of disease outbreak. It's easy to observe that in the absence of control strategies ($u_1(t) = u_2(t) = u_3 = 0$), the basic reproduction number; $R_0 = \max(0.63775,\ 1.7857) = 1.7857 > 1$ and the disease persisted. On the other hand, with maximum control strategies ($u_1(t) = u_2(t) = u_3(t) = 1$), the control reproduction $R_c = \max(0.0744,\ 0.2296) = 0.2296 < 1$, and transmission of the infection get reduced. In this case, observe that $R_c \leq R_0$ as theorized. Now, to understand in detail, we

plotted contour phase diagram of the corresponding control reproduction number R_c, against the intervention strategies $(u_1(t),\ u_2(t))$ as seen in figure 2 a. In figure 2 a, the diagram shows that any increase of both control strategies; educational intervention programmes $(u_1(t))$ and vaccination intervention $(u_2(t))$, lead to a corresponding decrease in reproduction number (R_c). Also, a contour phase diagram of basic reproduction number (R_0) in the absence of intervention controls in figure 2 b, shows otherwise.

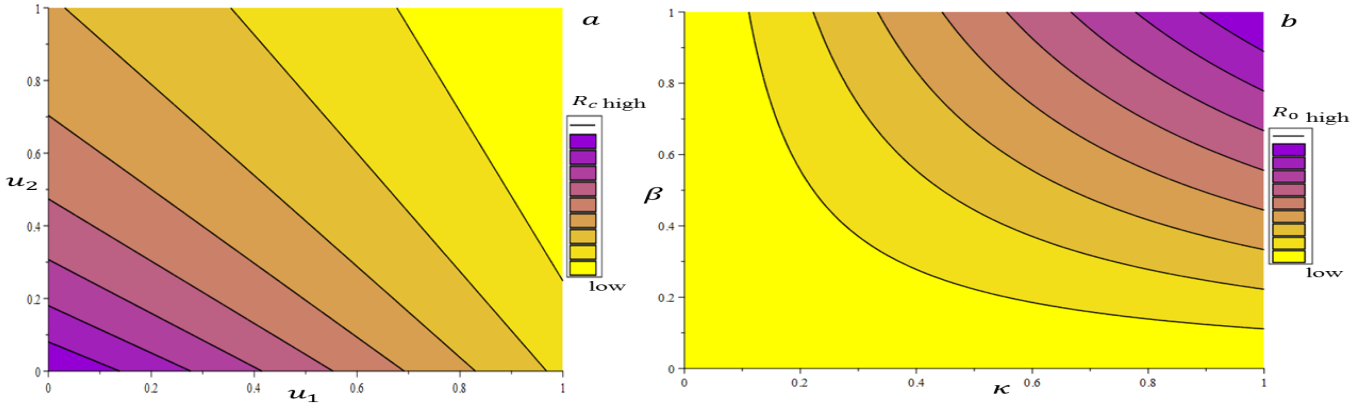

Figure 2: contour maps of impacts of controls on COVID-19 reproduction numbers; R_c and R_0

Hence adhering to educational awareness programmes on proper hygiene, usage of personal protective facilities, practicing of social distance, as well as getting vaccinated reduced the spread the infection.

4.20 Impacts of Control Interventions on Compartmental Subpopulations

Four possible control strategies were implemented in the model to assess optimal intervention in the model. These entails the plausible combinations of the three control measures; Educational programmes , vaccination, and treatment interventions respectively.

4.21 Strategy I: Control of COVID-19 using Educational programmes and Vaccinations

In the case, the combination of two control measures are implemented to curtail the spread of the infection $(u_1(t) \neq 0, u_2(t) \neq 0, u_3(t) = 0)$. These include creating robust awareness through educational programmes about utilization of safety measures such a practicing of social distancing, practicing of good personal hygiene, and usage of personal protective equipment. Also, the exposed class, asymptomatic infected class and infected are vaccinated, while restricting treatment for the hospitalized class.

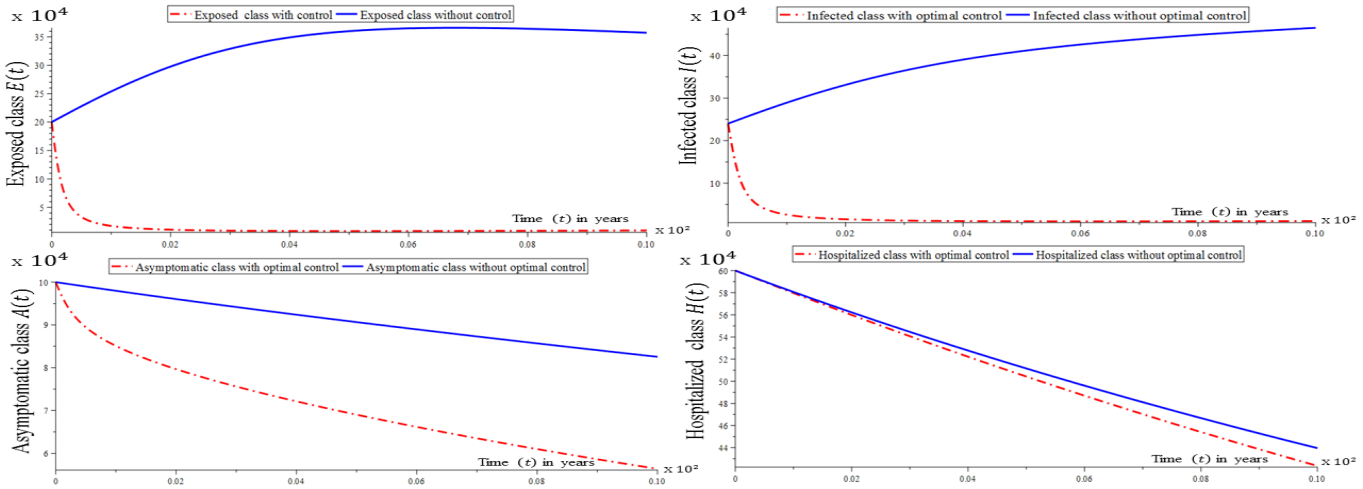

Figure 3: optimal control using strategy I $(u_1 \neq 0, u_2 \neq 0, u_3 = 0)$

Observe that in figure 3 (a), the control strategy steers and reduced the number of exposed class drastically toward zero. Similar behaviours are observed in figure 3 (b-d), where the subpopulation of asymptomatic infected, infected and hospitalized classes are reduced drastically when strategy I is applied. On the other hand, there is a corresponding increase in the number of the recovered individuals when strategy I is applied as seen in figure 4.

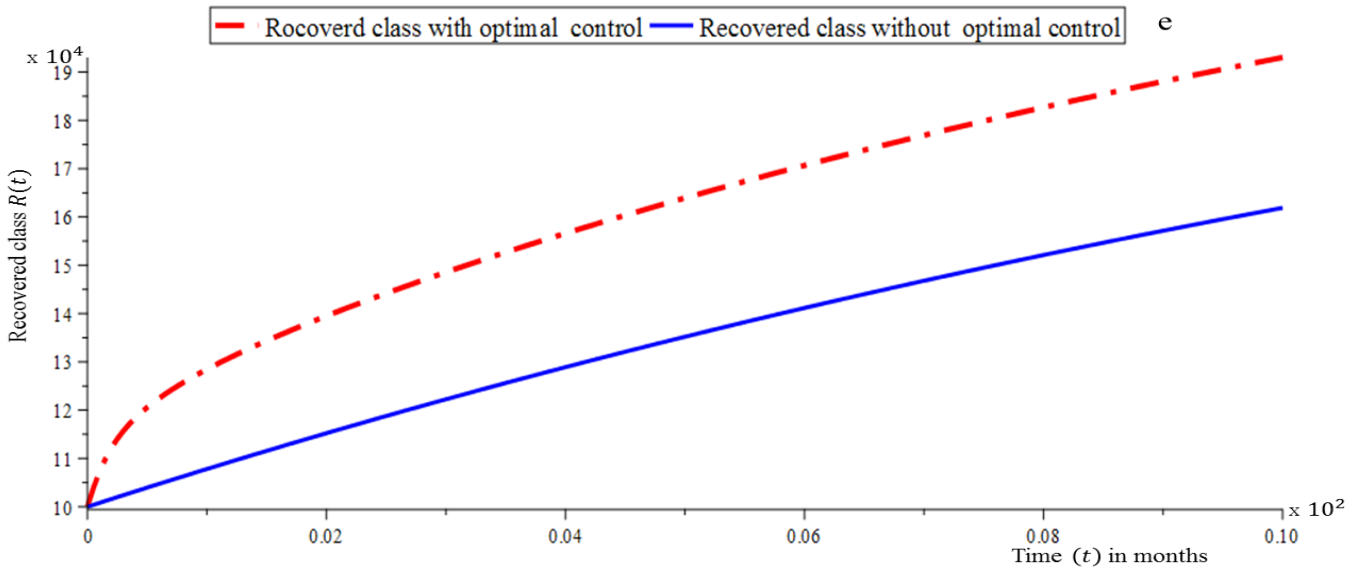

Figure 4: optimal control strategy I (recovered class)

4.22 Strategy II: Control of COVID-19 using Educational Programmes(EP) and Treatments

In figure 5 (a-d), this strategy depicts optimizing the educational intervention programmes for the entire population, and treatment of the hospitalized class, while vaccination is halted in the model $(u_1(t) \neq 0, u_2(t) = 0, u_3(t) \neq 0)$. Comparatively, using figure 5 a, the exposed class were still vulnerable until two and half (2.5) months later than that of strategy I of exactly two (2) months before down to zero level of exposure. In figure 5 b, one can observe that the optimal controls for strategy II might to be effective as the total number of infected individuals keep increasing exponentially, and above the total infected person before the intervention. In the same vein, figure 5 (c-d) shows a decrease in the population of the asymptomatic class, and hospitalized class among the population, when strategy II is being applied.

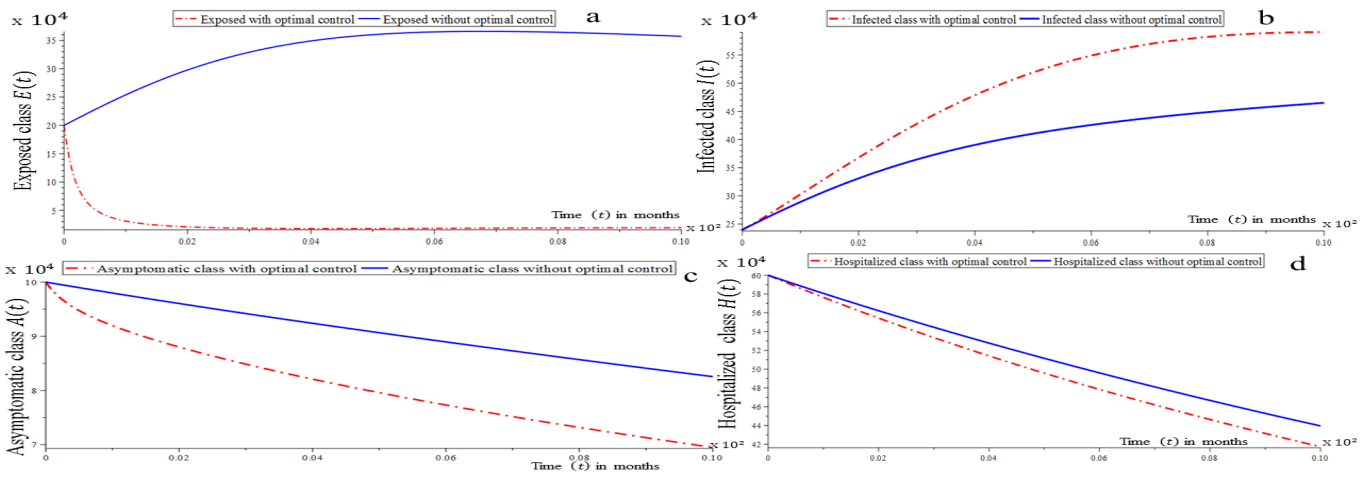

Figure 5: optimal control using strategy II $(u_1 \neq 0, u_2 = 0, u_3 \neq 0)$

In figure 6, inspite the continuous increase in the infected class, the recovered class keep increasing, because of treatment administered to the active cases in the hospital, but slower as compared to strategy I. This could likely attract the purchase of more cost-intensive health resources like intensive care facilities, more hospital bed-space, and more human personnel with additional cost. Hence the strategy II could be capital intensive during execution phase.

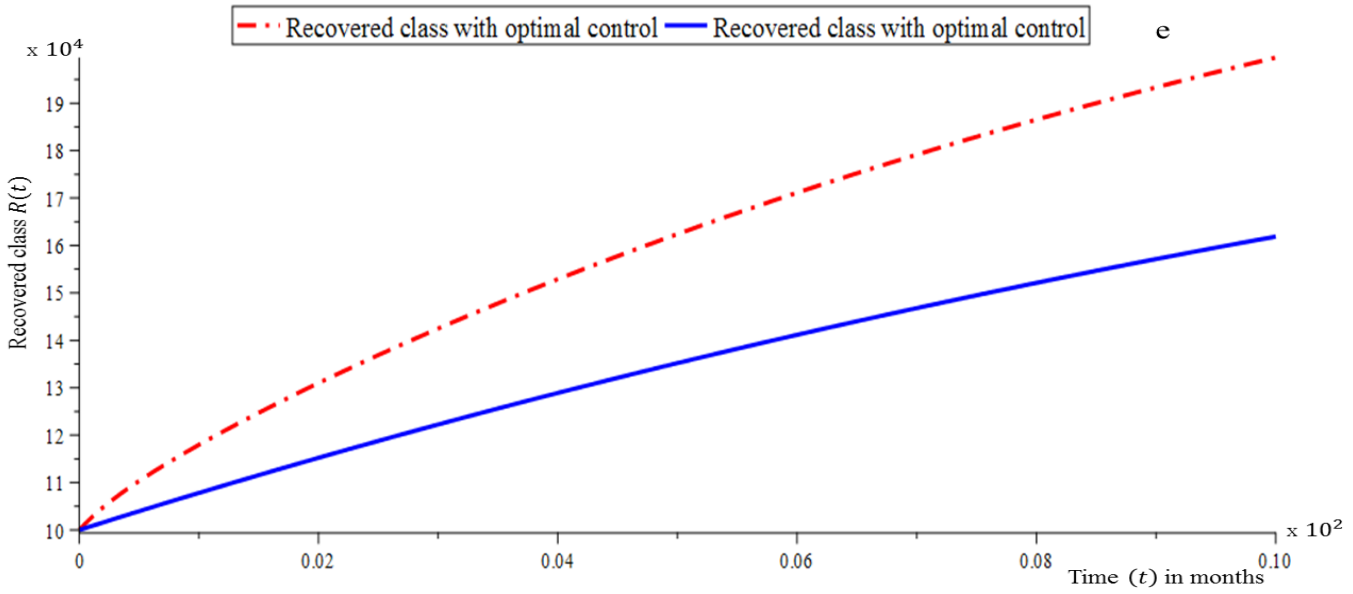

Figure 6: optimal control strategy II (recovered class)

4.23 Strategy III: Control of COVID-19 using Vaccinations and Treatments

In figure 7(a-d), the implementation of vaccination and treatment approaches are considered, in the absence of Educational intervention programmes ($u_1 = 0, u_2 \neq 0, u_3 \neq 0$). It was observed in figure 7 a, that there were increasing exposure of individuals to the infection after seven(7) months of intervention instead of decrease as anticipated. This was attributed to the fact that the exposed class may have lacked behind in proper Education and awareness on how to curtail the spread of the infection using non-pharmaceuticals. Similarly, although there was a drastic decrease in the number of the infected class, as seen in figure b, there was an infection relapse after two (2) months.

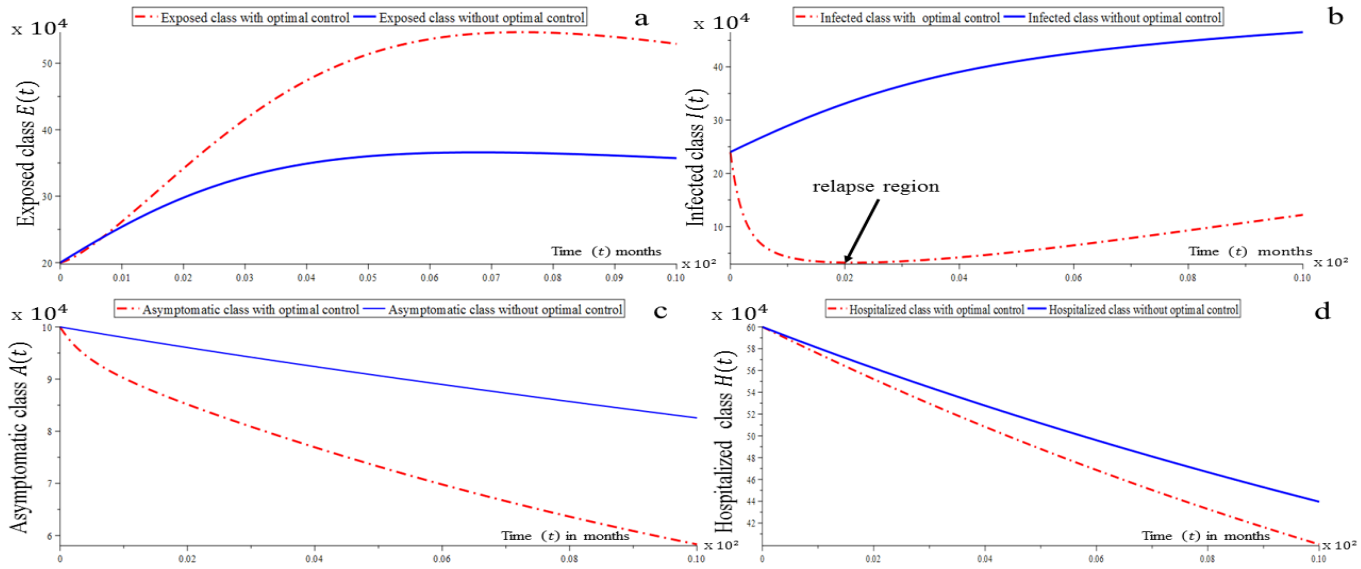

Figure 7: optimal control using strategy III ($u_1 = 0, u_2 \neq 0, u_3 \neq 0$)

Although there is increase in recovery subpopulation, as seen in figure 8, the occurrence of disease relapse rendered this strategy less effective as compared to other strategies. Its demonstrates re-emergence or development of a new variant of the disease as individuals may have failed to adhere to basic routine procedures of suppressing a new variant through educational sensitization and usage of protective wears.

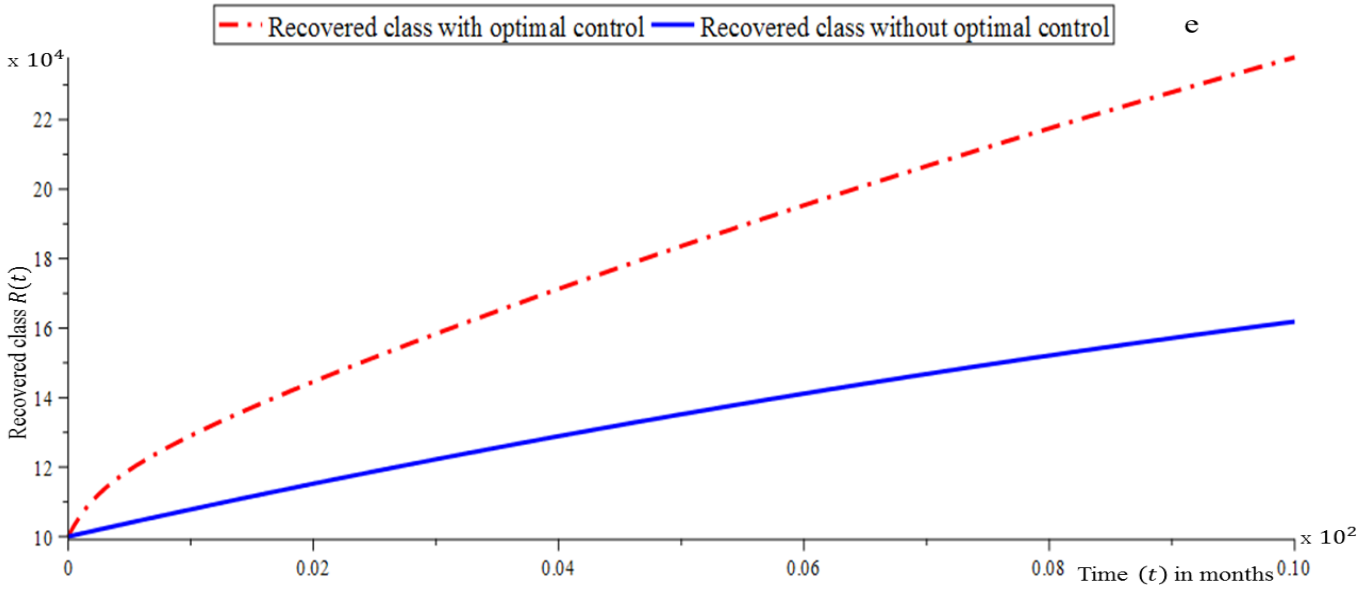

Fig. 8. Occurrence of disease relapse strategy

4. 24 Strategy IV: Control of COVID-19 using Education Programme, Vaccination and Treatment

This strategy requires implementing the three (3) control measures; Educational programmes, vaccinations, and treatment of the active cases ($u_1 \neq 0, u_2 \neq 0, u_3 \neq 0$) simultaneously. The dynamics of the model when simulated using this strategy possesses similar characteristics as compared to strategy I but varied in efficiency. So efficiency analysis(EA) helps to identify the intervention that prevents the highest number of infections in human population with no regard to the cost of control implementation. Thus an intervention with the highest efficiency index (EI), computed as

$$EI = \frac{\text{Total infection averted by intervention}}{\text{Total infection without intervention}} \times 100\%$$

is most efficient. The total infection averted by intervention is the difference between total infected individual without optimal control and the total infected individuals with optimal control. The model parameters remain the same, but the intervention cost weights were estimated as $B_1 = 20$, $B_2 = 25$, $B_3 = 55$. Table 3 is a summary of the efficiency indices of the four (4) control strategies, arrange in decreasing order after about four(4) months of intervention and infection relapsed time.

Table 3: Efficiency indices of control strategies

Control Strategy	Strategy I	Strategy IV	Strategy III	Strategy II
Efficiency(%)	96.0	91.0	89.0	-23.0

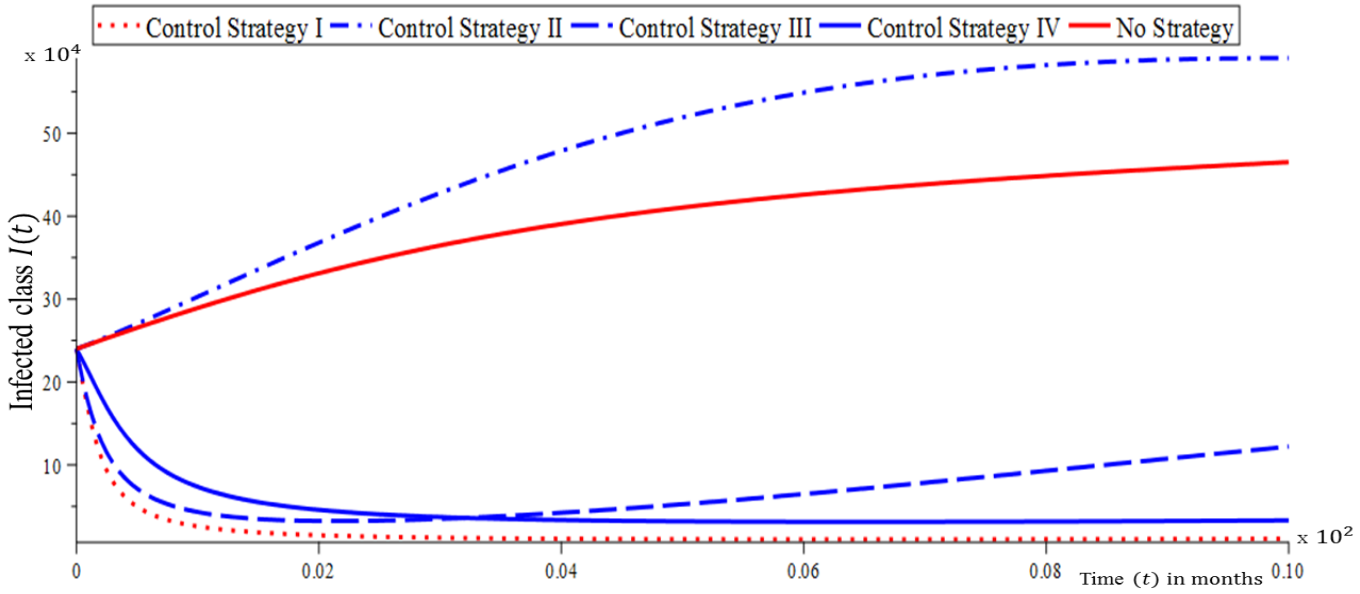

Figure 9: Efficiency profile of control strategies on infected class

Using the efficiency index in table 3, and its profile in figure 9, one can observed that strategy 1 is more efficient than others in reducing the total number of infected persons. On the other hand, strategy 2 performed poorly during the simulation time and seen to be highly inefficient as the number of infected class keeps increasing in the present of treatment. This in turn causing the infection to persist for a longer period of time. Hence embarking on flexible education programmes to create social awareness on proper sanitation, practicing of good personal hygiene, practicing social distancing, use of personal protective equipment and as well as getting the people vaccinated are efficient ways of controlling the spread of the infection in the community.

5.0 Conclusion

This model assesses the efficiency of optimal control strategies that was implemented to curtail the transmission of COVID-19 in Akwa Ibom state, Nigeria. It is formulated as an optimization problem consisting of six(6) compartmental subpopulations (susceptible, exposed, asymptomatic, infected, hospitalized and recovered) classses of individiuals. Three (3) control interventions(i.e flexible educational programmes, vaccinations and treatments) were coupled into the autonomous system of nonlinear differential equations. An optimzation cost functional with interest of the controls on exposed, infected and hospitialized classes was derived for the model, and characterized using optimal control theory. The qualitative properties of the model such as controllability, existence of extremal solutions, and characteristion of infection severity were established using some results in functional analysis, local stability conditions, and basic reproduction numbers of the virus. Epidemiological datasets generated from NCDC, validated and estimated in the literature were used to simulate the model parameters and state variables for a period of ten (10) months. A forward-backward iterative numerical solutions for the optimility system was aided by the maple16 software. The results shown that strategy 1 was more efficient that other strategies in reducing the number of infected person, and as a means to eradicate the infectious disease. Although the control function for treatment of the hospitalized was halted when strategy 1 was executed, the total cases of recovery keeps increasing. This could be attributed to the herds immunity in asymptomatic persons in the community. This model serve as an evaluation tool for the community health works, and other stakeholders. The study recommended a continuous vaccination and educational awareness campaign in the general public as tool to combat subsequent re-emergence of any other variant of corona virus and other infectious diseases.

References

[1] Afeez Abidemi. Optimal cost-effective control of drug abuse by students: insight from mathematical modeling. *Modeling Earth Systems and Environment*, 9(1):811–829, 2023.

[2] Isaac A Adedeji, Saheed Akinmayowa Lawal, and Sola Aluko-Arowolo. Qualitative analysis of coping strategies among older persons during covid-19 lockdown in nigeria: Considerations for community health promotion. *Community Health Equity Research & Policy*, page 2752535X231173527, 2023.

[3] JO Akanni. A non-linear optimal control model for illicit drug use and terrorism dynamics in developing countries with time-dependent control variables. *Decision Analytics Journal*, 8:100281, 2023.

[4] E. T Akpan, Enobong E Joshua, and E I Uduk. Nonlinear dynamics and synchronization of computational cognitive model in educational sciences. *J. Nonlinear Sci. Appl*, 14(1):15–28, 2020.

[5] Cicik Alfiniyah, Anisa Puspitasari, and Fatmawati Fatmawati. Mathematical modelling of drug abuse reduction strategies taking into account the treatment type and risks level. *Jambura Journal of Biomathematics (JJBM)*, 4(1):23–30, 2023.

[6] Joshua Kiddy K Asamoah, Eric Okyere, Afeez Abidemi, Stephen E Moore, Gui-Quan Sun, Zhen Jin, Edward Acheampong, and Joseph Frank Gordon. Optimal control and comprehensive cost-effectiveness analysis for covid-19. *Results in Physics*, 33:105177, 2022.

[7] Dimitri Breda, Toshikazu Kuniya, Jordi Ripoll, and Rossana Vermiglio. Collocation of next-generation operators for computing the basic reproduction number of structured populations. *Journal of Scientific Computing*, 85:1–33, 2020.

[8] Andrew F Brouwer. Why the spectral radius? an intuition-building introduction to the basic reproduction number. *Bulletin of Mathematical Biology*, 84(9):96, 2022.

[9] E. E. Joshua E. T. Akpan, U. G. Inyang. Mathematical modelling and computational dynamics of quasi-lockdown control of covid-19 pandemic in akwa ibom state, nigeria. *Journal of Mathematical Sciences and Modelling [JMSM, J. Math. Sci. Model. Monograph in Galley-Proof Stage]*, 2023.

[10] Wendell H Fleming and Raymond W Rishel. *Deterministic and stochastic optimal control*, volume 1. Springer Science & Business Media, 2012.

[11] RH Huang, DJ Liu, J Guo, JF Yang, JH Zhao, XF Wei, S Knyazeva, M Li, RX Zhuang, CK Looi, et al. Guidance on flexible learning during campus closures: Ensuring course quality of higher education in covid-19 outbreak. *Beijing: Smart Learning Institute of Beijing Normal University*, 2020.

[12] Enobong E Joshua and Ekemini T Akpan. Persistence and global dynamics of extended rosenzweig macarthur model. *Mathematical Theory and Modelling*, 6(8):85–99, 2016.

[13] Enobong E Joshua, Ekemini T Akpan, Olukayode Adebimpe, and CE Madubueze. Existence and uniqueness of positive periodic solution of an extended rosenzweig-macarthur model via brouwer's topological degree. *British Journal of Mathematics & Computer Science*, 20(4):1–10, 2017.

[14] Enobong E Joshua, Ekemini T Akpan, et al. Global stability and hopf-bifurcation analysis of biological systems using delayed extended rosenzweig-macarthur model. *Modern Applied Science*, 12(2):171–181, 2018.

[15] Temesgen Duressa Keno, Hana Tariku Etana, et al. Optimal control strategies of covid-19 dynamics model. *Journal of Mathematics*, 2023, 2023.

[16] Mark Grigor'evich Krein and Mark A Rutman. Linear operators leaving invariant a cone in a banach space.

[17] Legesse Lemecha Obsu and Shiferaw Feyissa Balcha. Optimal control strategies for the transmission risk of covid-19. *Journal of biological dynamics*, 14(1):590–607, 2020.

[18] Ifeoma Nkiruka Menakaya, Nnamdi Menakaya, Aderonke Adebowun Abah, and Gloria Okeoghenemaro Agboghoroma. Safety precaution and infection control practices among dental practitioners in nigeria during the covid-19 pandemic. *European Journal of Dental and Oral Health*, 4(2):14–20, 2023.

[19] Hengameh Mirhajianmoghadam and Mohammad-R. Akbarzadeh-T. Predictive hierarchical harmonic emotional neuro-cognitive control of nonlinear systems. *Engineering Applications of Artificial Intelligence*, 111:104781, 2022.

[20] Jayanta Mondal and Subhas Khajanchi. Mathematical modeling and optimal intervention strategies of the covid-19 outbreak. *Nonlinear Dynamics*, 109(1):177–202, 2022.

[21] Dennis Nordvall, Dan Drobin, Toomas Timpka, and Robert G Hahn. Co-morbidity associated with development of severe covid-19 before vaccine availability: a retrospective cohort study in the first pandemic year among the middle-aged and elderly in jönköping county, sweden. *BMC Infectious Diseases*, 23(1):1–6, 2023.

[22] S Olaniyi, OS Obabiyi, KO Okosun, AT Oladipo, and SO Adewale. Mathematical modelling and optimal cost-effective control of covid-19 transmission dynamics. *The European Physical Journal Plus*, 135(11):938, 2020.

[23] Adeola Yetunde Olukosi, Muinah Fowora, Adeniyi Kazeem Adeneye, Emelda Chukwu, Oluwagbemiga Aina, Olusola Ajibaye, Ayorinde James, Chidinma Gab-Okafor, Susan Abiodun Holdbrooke, Esther Ngozi Ohihoin, et al. A survey of chloroquine use for prevention and treatment of covid-19 in nigeria. *African Health Sciences*, 23(1):83–92, 2023.

[24] Andrew Omame, Mary Ele Isah, and Mujahid Abbas. An optimal control model for covid-19, zika, dengue, and chikungunya co-dynamics with reinfection. *Optimal Control Applications and Methods*, 44(1):170–204, 2023.

[25] BI Omede, UB Odionyenma, AA Ibrahim, and Bolarinwa Bolaji. Third wave of covid-19: mathematical model with optimal control strategy for reducing the disease burden in nigeria. *International Journal of Dynamics and Control*, 11(1):411–427, 2023.

[26] World Health Organization et al. Covid-19 weekly epidemiological update, edition 157, 1 sept, 2023. 2023.

[27] Mick G Roberts and JAP Heesterbeek. Characterizing the next-generation matrix and basic reproduction number in ecological epidemiology. *Journal of mathematical biology*, 66(4-5):1045–1064, 2013.

[28] Lionel Rosier. *Finite Dimensional Controllability*, pages 395–408. Springer New York, New York, NY, 2011.

[29] Pritam Saha, Sudhanshu Kumar Biswas, Md Haider Ali Biswas, and Uttam Ghosh. An seqaihr model to study covid-19 transmission and optimal control strategies in hong kong, 2022. *Nonlinear Dynamics*, 111(7):6873–6893, 2023.

[30] Fatima Saleh, David Idowu Olatunji, Ehichioya Ofeimun, Evaezi Okpokoro, Emily Crawford, Mahmood Dalhat, Ehimario Igumbor, Sunday Eziechina, Stella Inweregbu, Chinwe Lucia Ochu, et al. Epidemiology and psychosocial assessment of covid-19 among workers of the nigeria centre for disease control infected with covid-19. *Journal of Public Health in Africa*, 14(1), 2023.

[31] Luca Scarpa and Margherita Zanella. Degenerate kolmogorov equations and ergodicity for the stochastic allen–cahn equation with logarithmic potential. *Stochastics and Partial Differential Equations: Analysis and Computations*, pages 1–45, 2023.

[32] Heinz Schättler and Urszula Ledzewicz. Optimal control for mathematical models of cancer therapies. *An application of geometric methods*, 2015.

[33] Shikha Sharma, Rinkle Rani, and Nidhi Kalra. Genomic characterization of emerging sars-cov-2: A systematic review. *Current Bioinformatics*, 18(5):375–408, 2023.

[34] Muhammad Sher, Kamal Shah, Muhammad Sarwar, Manar A Alqudah, and Thabet Abdeljawad. Mathematical analysis of fractional order alcoholism model. *Alexandria Engineering Journal*, 78:281–291, 2023.

[35] Taiwo Oluwaseun Sokunbi, Abdmateen Temitope Oluyedun, Emmanuel Ayomide Adegboye, Glory Peace Oluwatomisin, and Abdulmumin Damilola Ibrahim. Covid-19 vaccination in nigeria: Challenges and recommendations for future vaccination initiatives. *Public Health Challenges*, 2(1):e57, 2023.

[36] Jie Sun, Sangahn Kim, and Fang Zhao. Mathematical modeling of optimal allocation of remote workforce: an interdisciplinary investigation with hofstede's cultural factors and managerial ability. *Cross Cultural & Strategic Management*, 30(2):219–247, 2023.

[37] Kosuke Takada, Mahoko Takahashi Ueda, Shintaro Shichinohe, Yurie Kida, Chikako Ono, Yoshiharu Matsuura, Tokiko Watanabe, and So Nakagawa. Genomic diversity of sars-cov-2 can be accelerated by mutations in the nsp14 gene. *Iscience*, 26(3), 2023.

[38] J Wauer, D Schwarzer, GQ Cai, and YK Lin. Dynamical models of love with time-varying fluctuations. *Applied Mathematics and Computation*, 188(2):1535–1548, 2007.